

Simultaneous type-0 and type-II spontaneous parametric down-conversions in a single periodically poled KTiOPO_4 crystal

H.J. Lee · H. Kim · M. Cha · H.S. Moon

Received: 21 February 2012 / Revised version: 19 April 2012 / Published online: 16 June 2012
© Springer-Verlag 2012

Abstract We demonstrate simultaneous type-0 and type-II spontaneous parametric down-conversions (SPDCs) in a single periodically poled KTiOPO_4 (KTP) crystal with a domain-inversion period of $10.00\ \mu\text{m}$. When a 45° linearly polarized 405 nm pump laser was injected into the crystal, the type-0 and the type-II SPDCs were simultaneously obtained using the third-order quasiphase matching (QPM) with the d_{33} and the first-order QPM with the d_{24} of KTP, respectively. We observed ring images due to the noncollinear propagation of the signals satisfying the three-dimensional type-0 and type-II QPM conditions, respectively. The observed results were in agreement with the calculated results based on the Sellmeier's formulas.

1 Introduction

Quantum entanglement has been considered as one of the most strikingly nonclassical features of quantum theory [1]. The optical sources of quantum entanglement have recently attracted attention since they have been used as the basic sources for quantum information technologies such as quantum teleportation, quantum cryptography, and quantum computing [2, 3]. Polarization-entangled photons are very useful for implementing entangled quantum bits since polarization is described by two orthogonal states which can

be easily measured and manipulated using only linear optical components. Polarization-entangled photons created by the spontaneous parametric down-conversion (SPDC) have been used in a wide range of experiments in quantum optics. In a SPDC process, a higher energy pump photon is split into a pair of lower energy photons inside the nonlinear crystal [4].

The efficiency of SPDC can be increased by employing some of the recent advances in nonlinear optics. Since quasi-phase matching (QPM) was proposed by Armstrong et al. [5], photon-pair generation with quasiphase-matched SPDC has become a feasible approach with periodically poled ferroelectric nonlinear crystals [6, 7]. SPDCs in the visible and near-IR spectral range have been practically implemented with periodically poled KTiOPO_4 (KTP) crystals by using UV laser diode (LD) pumps [8–10].

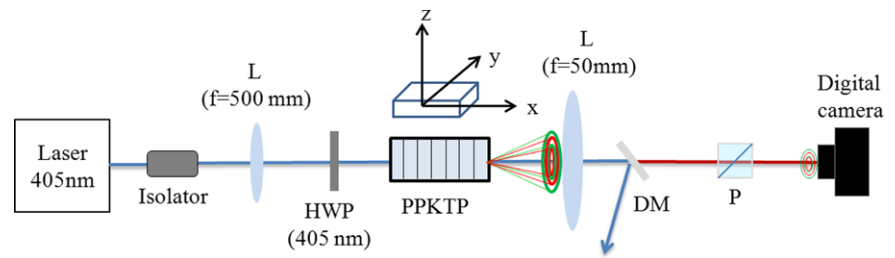
As is well known, either the type-0 or the type-II phase-matched SPDC can be used in a periodically poled KTP (PPKTP) crystal with a different grating period [6], which utilizes the largest diagonal nonlinear coefficient d_{33} (16.9 pm/V) or the off-diagonal coefficient, d_{24} (3.64 pm/V), respectively [11]. In the case of the type-0 SPDC, the QPM grating period is almost one-third of the type-II QPM grating period because the dispersion of KTP increases rapidly in the UV-blue region. SPDC in PPKTP has usually been performed using the type-II QPM [8–10].

There are several experiments related to multiple nonlinear effects in the same crystal. In [12] people demonstrated noncollinear double QPM, which is the simultaneous phase matching of two different nonlinear processes (second harmonic generation and third harmonic generation) in a single crystal. Jun Chen et al. [13] generated type-0 and type-II SPDC in PPKTP waveguide was designed to support type-0 SPDC. They also explained that type-II phase matching does not need any contribution from periodic poling and,

H.J. Lee · M. Cha · H.S. Moon (✉)
Department of Physics, Pusan National University, Busan
609-735, Korea
e-mail: hsmoon@pusan.ac.kr

H. Kim
Basic Science Research Institute, University of Ulsan,
Ulsan 680-749, Korea

Fig. 1 Schematic diagram of experimental setup for SPDCs in a PPKTP crystal with a violet 405 pump laser (L: lens, HWP: half-wave plate, DM: dichroic mirror, P: polarizer)



therefore, a variation in grating period will not affect the bandwidth of type-II SPDC, which results type-II SPDC is much brighter than type-0 SPDC.

In this paper, we have studied simultaneous generation of the type-0 and type-II noncollinear QPM SPDCs in a single PPKTP crystal with a pump at 405 nm. We observed two coexisting ring images of the SPDCs. The observations are based on separate tensor component (d_{33} and d_{24}) in the PPKTP crystal and explained by evaluating the QPM conditions for either first-order or third-order phase matching. We considered both type-II and type-0 QPM SPDC because the crystal was designed to produce type-II SPDC. In addition, we numerically calculated SPDCs of collinear and noncollinear using vectorial QPM conditions based on the Sellmeier's equation [14–17].

2 Experimental setup

Figure 1 shows the experimental setup for the generation of SPDC in PPKTP. The pump laser used for our experiment was an external-cavity LD laser operating at a wavelength in the range from 403.8 nm to 405.0 nm, with a cw-power of 40 mW. For our experiment, the pump laser power was adjusted to approximately 3 mW, from which we could observe clear SPDC images. The QPM structure of the PPKTP crystal (from Raicol crystals) was designed for the type-II SPDC with 405 nm pumping. The QPM grating vector was along the x -axis with a grating period of 10.00 μm . The dimensions of the PPKTP were $x = 10$ mm, $y = 2$ mm, and $z = 1$ mm. The crystal was placed in a temperature-controlled oven.

The pump laser was focused to a spot with a 32 μm -radius and propagated along the x -axis in the PPKTP crystal. The polarization of the pump laser was rotated by a half-wave plate (HWP) in order to investigate the effect of the pump laser polarization of the pump laser on the type-0 and the type-II SPDC signals. The SPDC signals generated in the PPKTP were collimated using a lens with a diameter of 5 cm and a focal length of 5 cm, and the ring images of the SPDC signals were detected using a digital camera in the visible region. The pump was separated from the signals and the idlers by using a dichroic mirror (DM). A polarizer placed before the digital camera was used to verify the polarization direction of the generated SPDC signals.

3 Experimental results & discussion

We calculated the wavelengths of the signal and idler photons collinearly generated via the type-II SPDC at 405.0 nm pump polarized along the y -axis as a function of the grating period at 40.0 $^{\circ}\text{C}$, as shown in Fig. 2(a). The grating period for collinear frequency-degenerate down-conversion is 10.00 μm and the wavelengths of the signal and idler are 810 nm. However, in the case of the type-0 SPDC, when the pump laser was at 403.8 nm polarized along the z -axis, the calculated wavelength of the signal and idler photons as a function of the grating period at the crystal temperature 89.3 $^{\circ}\text{C}$ are shown in Fig. 2(b). In this case, the grating period for the collinear frequency-degenerate down-conversion is 3.33 μm , which is completely different from that in the case of the type-II SPDC. The grating period (for 1st-order QPM) for the type-0 SPDC is one-third of that for the type-II SPDC under the given conditions in Fig. 2.

We observed the signals of SPDC for the visible region using a digital camera when the pump laser was at 403.8 nm polarized along the y -axis and the crystal temperature was 89.3 $^{\circ}\text{C}$. Figure 3(a) shows a photograph of the ring image of the 1st-order type-II SPDC signal utilizing the nonlinear coefficient tensor component d_{24} of KTP. We could not see the generated SPDC in the infrared (IR) region due to IR cutoff in digital cameras. The bright spots at the center of the ring images are due to the residual light of the pump laser leaking through the dichroic mirror. A ring image is made of a rainbow from red to green because noncollinear SPDC occurs at different angles depending on the signal/idler wavelengths and the dispersion of KTP crystal. No blue ring was observed. Although an IR SPDC ring image has been observed in a BBO crystal [18], SPDC ring images in the visible region in a PPKTP crystal have never been reported. We investigated the polarization direction of the generated SPDC signals using the polarizer placed before the digital camera of Fig. 1. The polarization of the signal is orthogonal to one of the idler.

However, when the polarization direction of the pump laser was changed to the z -axis, a new ring image with a reduced propagation angle was observed, as shown in Fig. 3(b). Intuitively, we did not expect SPDC with the pump laser with z -axis polarization, because the polarization direction of the pump laser for SPDC was fixed at the y -axis

Fig. 2 Calculated wavelength of the collinear SPDC as a function of 1st-order QPM grating period in (a) type-II SPDC (405.0 nm pump, 40.0 °C) and (b) type-0 SPDC (403.8 nm pump, 89.3 °C)

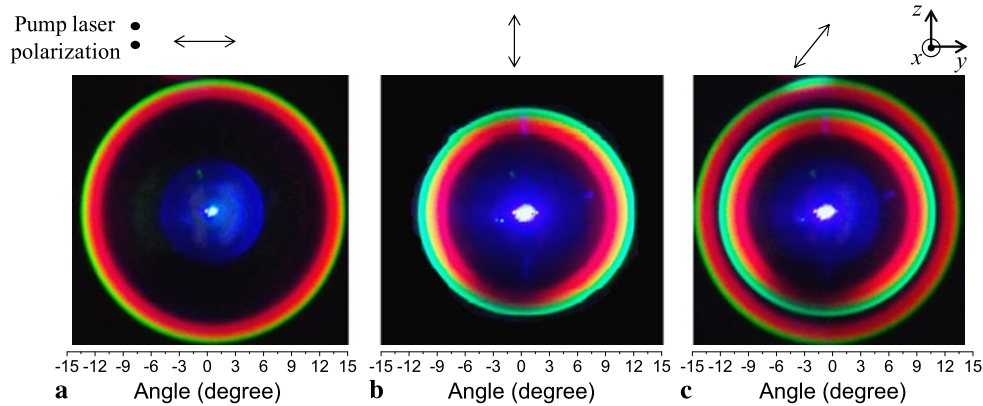
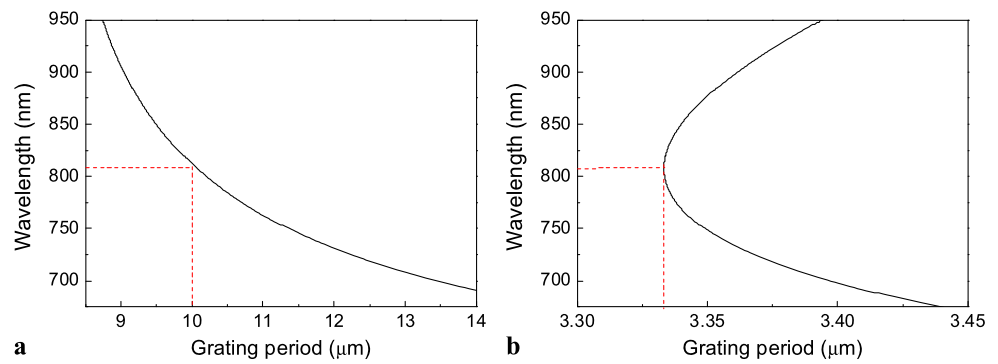


Fig. 3 Photographs of (a) ring image of the 1st-order type-II SPDC in the visible region, (b) ring image of the 3rd-order type-0 SPDC, and (c) ring images of the simultaneous generation of the 3rd-order type-0 and 1st-order type-II SPDCs. The arrows indicate the polarization di-

rections of the pump laser, and the bottom horizontal axes indicate the propagation angles of SPDC signals outside crystal, estimated from the measured radii of the ring images

in our type-II PPKTP crystal. We identify this new ring as the signal of the 3rd-order type-0 SPDC in the same PPKTP crystal originally designed for the type-II SPDC. It should be noted that during the ferroelectric domain inversion not only d_{24} , but also d_{33} changes sign in KTP crystals. Since the 1st-order grating period for the type-0 QPM is almost three times smaller than that for the type-II QPM, the 3rd-order type-0 SPDC is possible. The polarization of the signal is parallel to one of the idler.

In particular, when the pump laser was made 45° polarized, the two signal rings were simultaneously observed, as shown in Fig. 3(c). The dual rainbow ring images can be formed simply by merging the two ring images in Figs. 3(a) and (b). Although the effective nonlinear coefficient for the 3rd-order QPM is reduced by a factor of three, the nonlinear coefficient d_{33} (16.9 pm/V) is 4.6 times larger than the nonlinear coefficient d_{24} (3.64 pm/V) [11]. Comparing the intensities of the ring images in Fig. 3(c), we verified that the 3rd-order type-0 SPDC was more efficient than the 1st-order type-II SPDC. Therefore, the simultaneous generation of the type-0 and type-II SPDCs in a single crystal allows two polarization entanglement pairs generated from the single pump laser.

We investigated the polarization direction of the generated SPDC signals using the polarizer placed before the digital camera of Fig. 1. When we placed the polarizer at the output in the case of the 1st-order type-II SPDC, only one of the two photons (signal and idler) passed through it. When the polarizer was rotated by 90°, other photon was passed through it. In the case of the 3rd-order type-0 SPDC, all of the two photons passed through the polarizer. But when the polarizer was rotated by 90°, any photon was not passed through it.

In order to obtain measurable SPDC outputs, the QPM conditions must be satisfied: not only the total energy but also the total momentum (wave vector) of the photons must be conserved, including the QPM grating vector.

$$\omega_p = \omega_s + \omega_i, \tag{1}$$

$$\vec{k}_p = \vec{k}_s + \vec{k}_i + m\vec{K}_g \quad (m: \text{integer}), \tag{2}$$

$$|\vec{k}_j| = 2\pi \frac{n_j(\theta_j, T, \lambda_j)}{\lambda_j}, \tag{3}$$

where the subscripts $j = p, s, i$ denote the pump, signal and idler, respectively. ω_j is the angular frequency, \vec{k}_j is the wave vector, \vec{K}_g is the QPM grating vector ($K_g = \frac{2\pi}{\Lambda}$), m

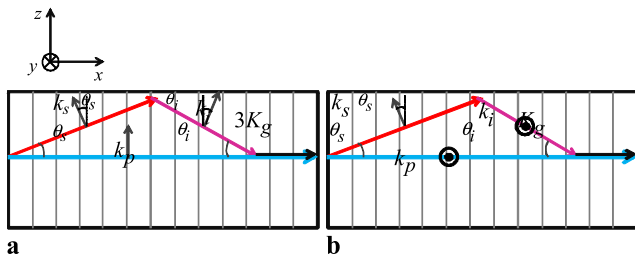


Fig. 4 Geometries for the noncollinear SPDCs in x - z plane of (a) type-0 SPDC (3rd-order QPM) and (b) type-II SPDC

is the QPM order, n_j is the index of refraction, and θ_j is the angle from z -axis.

The QPM condition is different, depending on whether QPM is of type-0 or type-II SPDC, because of the different dispersions for the principal indices in KTP. Let us consider the polarization configurations of the type-0 and type-II SPDCs in the x - z plane. For the type-0 QPM as shown in Fig. 4(a), the pump is polarized along the z -axis, and the signal and the idler are polarized in the x - z plane, making angles of θ_s and θ_i , respectively. In the case of type-II QPM in Fig. 4(b), the pump and idler are polarized along the y -axis, and the signal is polarized in the x - z plane, making an angle of θ_s from the z -axis. The polarization configurations in the x - y plane can be discussed in the same way (not shown).

Our experimental results were verified by numerically calculating the QPM conditions based on the Sellmeier’s equations for the principal indices [14–17]. For example, in the case of the polarization configuration of the 3rd-order type-0 QPM in the x - z plane, as shown in Fig. 4(a), the QPM conditions in Eqs. (1) and (2) become

$$\frac{1}{\lambda_p} = \frac{1}{\lambda_s} + \frac{1}{\lambda_i}, \tag{4}$$

$$k_s \cos \theta_s + k_i \cos \theta_i = k_p - 3K_g, \tag{5}$$

$$k_s \sin \theta_s = k_i \sin \theta_i, \tag{6}$$

where θ_s and θ_i are the angles of \vec{k}_s and \vec{k}_i with respect to the pump wave vector \vec{k}_p (along the x -axis), respectively. The refractive indices of the signal and the idler in the x - z plane are expressed as

$$n_{s(i)}(\theta_{s,i}, T, \lambda_{s,i}) = \frac{n_x(T, \lambda_{s(i)})n_z(T, \lambda_{s(i)})}{\sqrt{n_x^2(T, \lambda_{s(i)}) \cos^2 \theta_{s(i)} + n_z^2(T, \lambda_{s(i)}) \sin^2 \theta_{s(i)}}}, \tag{7}$$

where $n_{s(i)}$ is the refractive index of the signal or idler as a function of the angle $\theta_{s(i)}$, the crystal temperature T , and the wavelength of the signal or idler $\lambda_{s(i)}$. When θ_s and θ_i are small (near-collinear condition), $n_{s(i)}$ is approximately n_z . The refractive index of the pump is $n_p = n_y(T, \lambda_p)$. These indices determine k_j ’s in Eqs. (5) and (6).

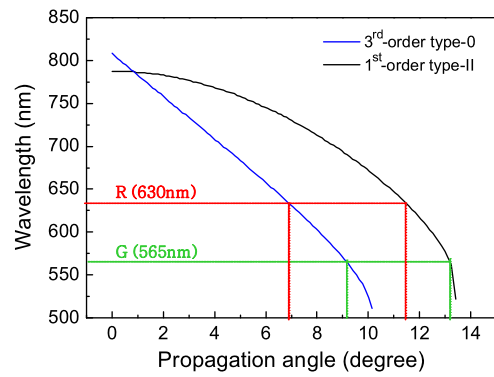


Fig. 5 Calculated signal wavelength as a function of external propagation angle for the 3rd-order type-0 (blue curve) and the 1st-order type-II SPDCs (black curve). The propagation angles for the red and green rings are indicated as lines indicated as “R” and “G,” respectively

Also, in the case of the polarization configuration of the 1st-order type-II noncollinear SPDC in Fig. 4(b), the momentum conservation is satisfied by Eq. (2)

$$k_s \cos \theta_s + k_i \cos \theta_i = k_p - K_g, \tag{8}$$

$$k_s \sin \theta_s = k_i \sin \theta_i. \tag{9}$$

The refractive indices are given by

$$n_s(\theta_s, T, \lambda_s) = \frac{n_x(T, \lambda_s)n_z(T, \lambda_s)}{\sqrt{n_x^2(T, \lambda_s) \cos^2 \theta_s + n_z^2(T, \lambda_s) \sin^2 \theta_s}}, \tag{10}$$

$n_i = n_y(T, \lambda_i)$, and $n_p = n_y(T, \lambda_p)$ to be used in Eqs. (8) and (9).

To account for the simultaneous generation of the 3rd-order type-0 and 1st-order type-II SPDCs, we numerically calculated the phase-matched signal wavelength as a function of external propagation angle, in each case as shown in Fig. 5. The black curve shows the signal wavelength and external propagation angle for the 1st-order type-II SPDC. The blue curve shows the calculated results for the 3rd-order type-0 SPDC. We used the experimental conditions corresponding to Fig. 3 to determine the parameters for the numerical calculation in Fig. 5: the crystal temperature of $T = 89.3$ °C, the pump wavelength of 403.8 nm, and the grating period of 10.00 μm . The calculated propagation angle has been converted to the external angle in Fig. 5, according to Snell’s law.

As the wavelength of the signal photon decreases, the external propagation angle increases. The calculated propagation angles of the rings in Fig. 5 explain the experimental results in Fig. 3 quantitatively. The calculated QPM conditions of the type-0 and type-II SPDCs are not satisfied at the signal wavelengths shorter than 511 nm and 522 nm, respectively. This explains the blue cut-off (only red ~ green

rainbows) in Fig. 3. The theoretical results for the propagation angles are in good agreement with the observed results in Fig. 3, as indicated by the lines for green and red colors.

We estimated the efficiency of the type-II SPDC from photon counting results of the signal and idler photons under the condition of collinear interaction ($810 \text{ nm} \pm 5 \text{ nm}$). The conversion efficiency (η) is defined as the SPDC photon pair production rate per pump photon and described as follows [19]:

$$\eta = \frac{S_1 \cdot S_2}{R_C \cdot N_P}, \quad (11)$$

where S_1 and S_2 denote the net single count rates of the signal and idler photons, respectively. R_C and N_P are the net coincidence count rate and the count rate of the pump photon, respectively. In our experiment under the condition of collinear ($810 \text{ nm} \pm 5 \text{ nm}$), the net single count rates S_1 (signal) and S_2 (idler) were measured to be 45 kHz and 40 kHz, respectively. The net coincidence rate R_C without accidental coincidences was measured to be 3.1 kHz. Also, the pump photon count rate is estimated to be $6.1 \times 10^{15} \text{ Hz}$ from the pump power of 3.0 mW (405 nm). From Eq. (11), η is estimated to be 9.5×10^{-11} .

4 Conclusion

We demonstrated the simultaneous generation of the type-0 and type-II SPDCs in a PPKTP crystal. When a 45° linearly polarized diode laser was pumped into the PPKTP crystal, the type-0 and type-II SPDCs were simultaneously generated via 3rd-order type-0 QPM and 1st-order type-II QPM, respectively. We observed two coexisting ring images of the noncollinear type-0 and type-II SPDC signals in the visible region. Although the effective nonlinear coefficient for the 3rd-order QPM is 1/3 of the 1st-order QPM, the 3rd-order type-0 SPDC was more efficient than the 1st-order type-II SPDC because the nonlinear coefficient d_{33} was 4.6 times larger than the nonlinear coefficient d_{24} . The simultaneous generation of the type-0 and type-II SPDCs was calculated from the Sellmeier's equations, showing good agreement

with the observed ring images. The simultaneous generation of the type-0 and type-II SPDCs in a single crystal allowed two polarization entanglement pairs generated from the single pump laser. Our results are expected to help the generation of entangled multiphotons in a single crystal.

Acknowledgements This research was supported by Basic Science Research Program through the National Research Foundation of Korea (NRF) funded by the Ministry of Education, Science and Technology (Grant Nos. 2009-0070668 and 2012R1A2A1A01006579). M. Cha acknowledges the support by the National Research Foundation of Korea (Grant No. 2009-0068995).

References

1. A. Einstein, B. Podolsky, N. Rosen, *Phys. Rev.* **47**, 777 (1935)
2. A.K. Ekert, *Phys. Rev. Lett.* **67**, 661 (1991)
3. J.I. Cirac, A.K. Ekert, S.F. Huelga, C. Macchiavello, *Phys. Rev. A* **59**, 4249 (1999)
4. D. Klyshko, *Photons and Nonlinear Optics* (Gordon and Breach, New York, 1988)
5. J.A. Armstrong, N. Bloembergen, J. Ducuing, P.S. Pershan, *Phys. Rev.* **127**, 1962 (1918)
6. M. Fejer, G.A. Magel, D.H. Jundt, R.L. Byer, *IEEE J. Quantum Electron.* **28**, 2631 (1992)
7. M. Yamada, N. Nada, M. Saitoh, K. Watanabe, *Appl. Phys. Lett.* **62**, 435 (1993)
8. C.E. Kuklewicz, M. Fiorentino, G. Messin, F.N.C. Wong, J.H. Shapiro, *Phys. Rev. A* **69**, 013807 (2004)
9. M. Fiorentino, C. Kuklewicz, F. Wong, *Opt. Express* **13**, 127 (2005)
10. M. Fiorentino, R.G. Beausoleil, *Opt. Express* **16**, 20149 (2008)
11. H. Vanherzeele, J.D. Bierlein, *Opt. Lett.* **17**, 982 (1992)
12. T. Ellenbogen, A. Arie, S.M. Seltiel, *Opt. Lett.* **32**, 262 (2007)
13. J. Chen, A.J. Pearlman, A. Ling, J. Fan, A. Migdall, *Opt. Express* **17**, 6727 (2009)
14. T.Y. Fan, C.E. Huang, B.Q. Hu, R.C. Eckardt, Y.X. Fan, R.L. Byer, R.S. Feigelson, *Appl. Opt.* **26**, 2390 (1987)
15. F. Konig, F.N.C. Wong, *Appl. Phys. Lett.* **84**, 1644 (2004)
16. K. Fradkin, A. Arie, A. Skliar, G. Rosenman, *Appl. Phys. Lett.* **74**, 914 (1999)
17. W. Wiechmann, S. Kubota, T. Fukui, H. Masuda, *Opt. Lett.* **18**, 1208 (1993)
18. P.G. Kwiat, K. Mattle, H. Weinfurter, A. Zeilinger, A.V. Sergienko, Y.H. Shih, *Phys. Rev. Lett.* **75**, 4337 (1995)
19. S. Tanzilli, H. De Riedmatten, W. Tittel, H. Zbinden, P. Baldi, M. De Micheli, D.B. Ostrowsky, N. Gisin, *Electron. Lett.* **37**, 26 (2001)